Front. Phys., 2012, 7(3): 319–323
DOI 10.1007/s11467-011-0191-2

RESEARCH ARTICLE

Enhanced scattering of acoustic waves at interfaces

Li Zhao (赵瓅)[1], **Bin Liu** (刘斌)[1], **Yin-hao Gao** (高银浩)[2], **Yan-jiao Zhao** (赵艳皎)[3,*], **Ji-ping Huang** (黄吉平)[1,†]

[1] *Department of Physics and State Key Laboratory of Surface Physics, Fudan University, Shanghai 200433, China*
[2] *School of Machinery and Electricity, Henan Institute of Science and Technology, Xinxiang 453003, China*
[3] *Advanced Materials Laboratory, Fudan University, Shanghai 200438, China*
*E-mail: *zhaoyanjiao@fudan.edu.cn, †jphuang@fudan.edu.cn*
Received June 10, 2011; accepted June 20, 2011

We propose a general method to realize a total scattering of an incident acoustic wave at interfaces between different media while allowing the flow of air, fluids and/or particles. This originates from the enlargement of the equivalent acoustic scattering cross section of an embedded object coated with acoustic metamaterials, which causes the coated object to behave as a scatterer bigger than its physical size. We theoretically design a model circular cylindrical object coated with such metamaterials whose properties are determined according to two different, but identical, methods. The desired function is confirmed for both far-field and near-field cases with full wave simulations based on the finite element method. This work reveals a promising way to achieve noise shielding and naval camouflage.

Keywords superscattering, acoustic waves, finite element simulations

PACS numbers 43.20.+g, 43.35.+d, 43.40.+s

1 Introduction

Since 2006 electromagnetic cloaks have received extensive attention because of their potential applications [1–10]. Based on the concept of complementary media, Ma and his coworkers successfully proposed a novel design which can enlarge the electromagnetic wave scattering cross section of an object so that it looks like a scatterer bigger than its physical size [11–13]. Such an electromagnetic superscatterer was elaborately designed by coating an electromagnetic metamaterial with negative refractive index on a perfect electrical conductor cylinder [11, 12, 14]. Strictly following the concept of electromagnetic superscatterers, in this work we attempt to achieve a new type of acoustic superscatterers by using acoustic metamaterials with novel properties as to be determined. Although it is a straightforward extension of the similar mechanism for electromagnetic waves into acoustic waves, it still carries merits for acoustic applications, which might be easier to implement than for the electromagnetic wave case.

Acoustic metamaterials [15–27] have extended the realm of elastic wave characteristics achievable by phononic crystals and natural materials. In particular, composites with negative dynamic mass densities [20, 21] have demonstrated significantly subwavelength attenuation of sound in the audible regime by breaking the mass density law [15, 16]. In principle, acoustic metamaterials with the novel properties required for our proposed acoustic superscatterers can be designed by using local resonances [20, 21, 28].

In this work, we shall propose an accurate theoretical design of acoustic superscatterers in circular cylindrical cases, and confirm the desired function for both far-field and near-field cases with full wave numerical simulations based on the finite element method. Two different theoretical methods will be adopted, and the resulting equations derived from them agree with each other. Such acoustic superscatterers are potentially important for noise shielding and naval camouflage.

2 Theory

2.1 Method I

Let us start by considering a two-dimensional circular cylindrical object coated with acoustic metamaterials. Figure 1 is the schematic demonstration. Initially,

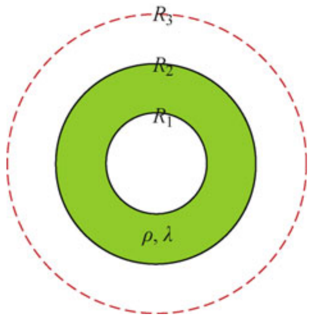

Fig. 1 Schematic graph showing a circular cylindrical acoustic superscatterer by coating a shell (inner radius: R_1; outer radius: R_2) of acoustic metamaterials (relative mass density tensor: ρ; relative bulk modulus: λ) to a small uniform cylinder of the radius R_1. The designed superscatterer of the physical outer radius R_2 responds to an incident acoustic wave as if its scattering cross section is the same as that of a virtual uniform cylinder with a physical radius R_3 (*dashed circle*). For the superscatterers investigated in Figs. 2–5, the region with a radius larger than R_2 can be filled with either uniform materials (e. g., air or water) or equivalently uniform materials (e. g., suspensions containing suspended particles with a scattering cross section much smaller than the wavelength of an incident acoustic wave), which can transmit acoustic waves (almost) without scattering. (Throughout this work, we are not considering the absorption of acoustic waves). And the region with a radius smaller than R_1 can be filled with any materials since the acoustic wave cannot penetrate the sound-soft boundary at R_1.

we consider a uniform cylinder with radius R_3 and a sound-soft boundary surface. Then we compress the uniform cylinder into a small one with radius R_1, with the sound-soft boundary condition unchanged. In order to accomplish such a compression, a pair of complementary media is introduced at the annulus between R_1 and R_3. The cylindrical interface between the two types of complementary media is denoted by its radius R_2. The region between R_2 and R_3 contains the same medium as that beyond R_3. The shell between R_1 and R_2 is filled with an acoustic metamaterial, whose properties are determined by Eqs. (5)–(8) below. The scattering ability of the designed object with outer radius R_2 for incident acoustic waves can be equivalent to that of the uniform cylinder with radius $R_3(> R_2)$, as to be displayed in Figs. 2 and 3. For simplicity, let us consider a continuous map between the pair of complementary media: The region between R_2 and R_3 is mapped to the shell of acoustic metamaterials, with R_3 to R_1 and R_2 to itself. The mapping can be recorded as a coordinate transformation between the original cylindrical mesh (r, θ, z) and the new mesh (r', θ', z'):

$$r' = -\frac{R_2 - R_1}{R_3 - R_2} r + \frac{R_3 - R_1}{R_3 - R_2} R_2 \tag{1}$$

$$\theta' = \theta \tag{2}$$

$$z' = z \tag{3}$$

Apparently, the anisotropic mass density tensor and bulk modulus in the shell can be readily obtained by the coordinate transformation method. However, since the basis vectors that result from a cylindrical transformation are not the usual cylindrical unit vectors, certain components need to be renormalized by using the length of these basis vectors. Schurig *et al.* [29] introduced a

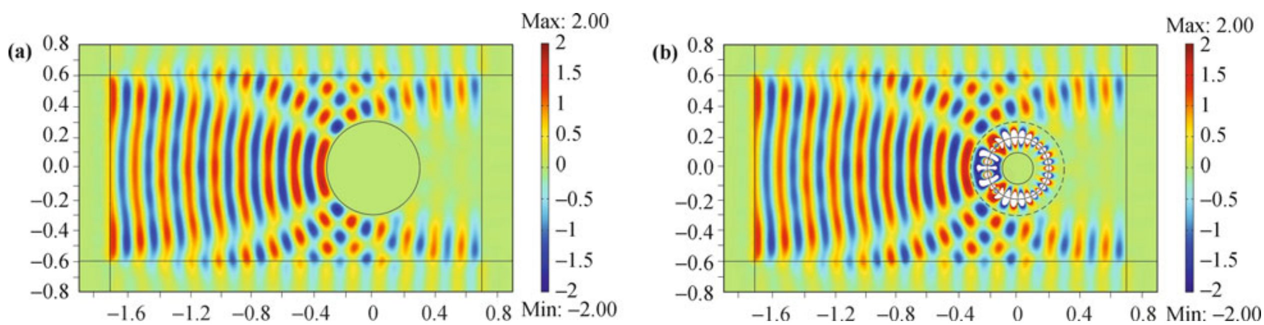

Fig. 2 Snapshot of the distribution of the pressure field induced by an incident acoustic plane wave (corresponding to far-field cases) with unit amplitude and frequency of 2000 Hz. **(a)** The pressure field distribution caused by a uniform circular cylinder of the radius $R_3 = 0.3$ m; **(b)** The pressure field distribution induced by the designed circular cylinder or acoustic superscatterer of an outer radius R_2, for $R_1 = 0.1$ m and $R_2 = 0.2$ m. The dotted circle indicates a virtual uniform cylinder with the radius $R_3 = 0.3$ m. It is shown that being beyond the virtual cylinder, the pressure field distribution is (almost) identical with that in the upper panel. The unit for both the x and y axes of Figs. 2–5 is meter.

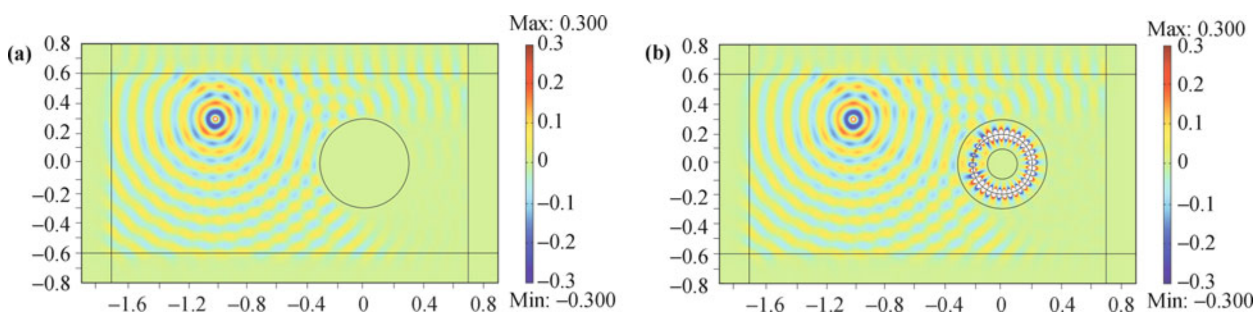

Fig. 3 The same as Fig. 2, but for an incident cylindrical wave (corresponding to near-field cases) with unit amplitude and frequency of 3000 Hz, the source of which is located at (–1 m, 0.3 m).

practical method to obtain the crucial Jacobian transformation matrix

$$(\Lambda_{i'j})=\begin{vmatrix} \frac{r'}{r}-R_2\frac{x^2}{r^3} & -R_2\frac{xy}{r^3} & 0 \\ -R_2\frac{xy}{r^3} & \frac{r'}{r}-R_2\frac{y^2}{r^3} & 0 \\ 0 & 0 & 1 \end{vmatrix} \tag{4}$$

According to the Eqs. (26) and (29) of Ref. [23], a straightforward derivation gives the relative (or renormalized) mass density tensor ρ and the relative (or renormalized) bulk modulus λ of the shell as

$$\rho_{x'x'}=-\frac{(R_3-R_2)^2r'^2\cos^2\theta'+\Delta^2\sin^2\theta'}{(R_3-R_2)r'\Delta} \tag{5}$$

$$\rho_{x'y'}=\rho_{y'x'} = -\frac{R_2(R_3-R_1)\sin\theta'\cos\theta'[r'(R_3-R_2)-\Delta]}{(R_3-R_2)r'\Delta} \tag{6}$$

$$\rho_{y'y'}=-\frac{(R_3-R_2)^2r'^2\sin^2\theta'+\Delta^2\cos^2\theta'}{(R_3-R_2)r'\Delta} \tag{7}$$

$$\lambda=-\frac{(R_2-R_1)^2r'}{(R_3-R_2)\Delta} \tag{8}$$

where

$$\Delta=R_2(R_3-R_1)-(R_3-R_2)r' \tag{9}$$

2.2 Method II

Alternatively, there is another way to obtain the material parameters of the shell. This method is analogous to that for dealing with electromagnetic superscatterers established in Ref. [11] due to the existence of mathematical similarity. To proceed, let us write the acoustic equation in the cylindrical coordinates (r, θ, z) as

$$\begin{pmatrix} \frac{\partial}{\partial r} & \frac{1}{r}\frac{\partial}{\partial\theta} & \frac{\partial}{\partial z}\end{pmatrix}\begin{pmatrix} \frac{1}{\rho_r} & & \\ & \frac{1}{\rho_\theta} & \\ & & \frac{1}{\rho_z}\end{pmatrix}\begin{pmatrix}\frac{\partial p}{\partial r} \\ \frac{1}{r}\frac{\partial p}{\partial\theta} \\ \frac{\partial p}{\partial z}\end{pmatrix} + \frac{\omega^2}{\lambda(x)}p(x)=0 \tag{10}$$

Since the pressure field p is a constant along the z-coordinate, we obtain the partial differential equations for p as

$$\lambda(x)\frac{1}{r}\frac{\partial}{\partial r}\left(\frac{r}{\rho_r}\frac{\partial p}{\partial r}\right)+\lambda(x)\frac{1}{r^2}\frac{\partial}{\partial\theta}\left(\frac{1}{\rho_\theta}\frac{\partial p}{\partial\theta}\right)+\omega^2p(x)=0 \tag{11}$$

Comparing it with Eq. (2) in Ref. [11], namely,

$$\frac{1}{\epsilon_z}\frac{1}{r}\frac{\partial}{\partial r}\left(\frac{r}{\mu_\theta}\frac{\partial E_z}{\partial r}\right)+\frac{1}{\epsilon_z}\frac{1}{r^2}\frac{\partial}{\partial\theta}\left(\frac{1}{\mu_r}\frac{\partial E_z}{\partial\theta}\right)+k_0^2E_z=0 \tag{12}$$

we may identify that these two equations [Eqs. (11) and (12)] are isomorphic by making the following variable exchanges

$$\lambda(x)\Leftrightarrow\frac{1}{\epsilon_z},\quad \rho_r\Leftrightarrow\mu_\theta,\quad \text{and}\quad \rho_\theta\Leftrightarrow\mu_r$$

Regarding the physical meaning of the parameters used in Eq. (12), please refer to Ref. [11] for the sake of clarity. Then the solution from the Mie scattering theory for electromagnetic superscatterers [11] subjected to an incident transverse-electric polarized electromagnetic field can also be applied to the design of the cylindrical acoustic superscatterers. Eventually, the derivation gives exactly the same expressions as Eqs. (5)–(8). Nevertheless, the first method involves much less derivations, and can be considered as a general routine for any geometric configurations.

3 Simulation results

Now we are in a position to present the simulation results of pressure field distributions calculated by the finite element method implemented in the commercial software COMSOL Multiphysics 3.5. In the simulations as depicted in Figs. 2–5, perfect matched layers are used to surround the central simulation area, which absorb the reflected waves. In Fig. 2, to mimic a far-field case, an acoustic plane wave is incident from left to right with unit amplitude and frequency of 2000 Hz. Figure 2(a) shows a uniform cylinder with the radius $R_3 = 0.3$ m and a sound-soft boundary surface, which is placed at the origin. In Fig. 2(b), a small uniform cylinder of He radius $R_1 = 0.1$ m with a sound-soft boundary surface is placed at the origin. And it is coated with a shell of acoustic metamaterials, whose outer radius is $R_2 = 0.2$ m. The material parameters, ρ and λ, of the shell is determined according to Eqs. (5)–(8), to enable an equivalently virtual cylinder with the radius $R_3 = 0.3$ m, as indicated by the dotted circle. Figure 2 displays the pressure field distribution induced by the incident plane wave and the reflected wave in the presence of a real uniform cylinder with the radius R_3 (upper panel) and a designed cylinder with the outer radius R_2 (lower panel). The function of the cylindrical acoustic superscatterer, namely, the designed cylinder, is well confirmed by comparing the pressure field distribution within the region of a radius $\geqslant 0.3$ m in the two panels. That is, the equivalent scattering cross section of the designed superscatterer with the physical outer radius R_2 is identical to that of the uniform cylinder of the radius $R_3(> R_2)$. In other words, our design can also enhance the acoustic wave scattering cross section of an object so that it responds as a scatterer bigger than its physical size. Similar results appear for the case of an incident cylindrical acoustic wave, which corresponds to a near-field case, as shown in Fig. 3.

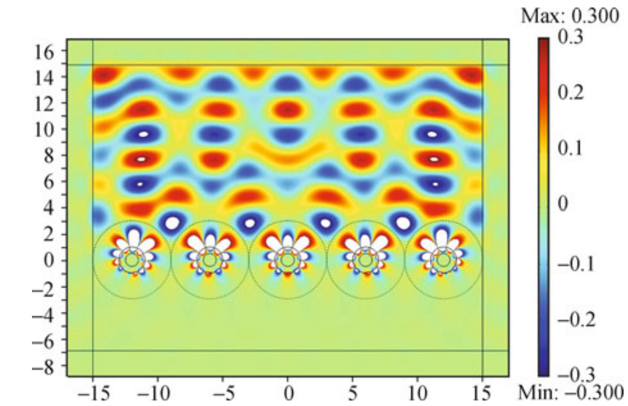

Fig. 4 Snapshot of the distribution of the pressure field induced by an incident acoustic plane wave with unit amplitude and frequency of 100 Hz in the presence of a line of five designed superscatterers. The locations of the superscatterers are purposefully selected so that the resulting virtual uniform cylinders with the radius R_3 (as indicated by the dotted circles) are exactly tangent to their neighbors. It is displayed that the acoustic wave is almost totally reflected such that the pressure field on the other side is nearly zero (or small enough to be neglected). Parameters: $R_1 = 0.5$ m, $R_2 = 1$ m, and $R_3 = 3$ m.

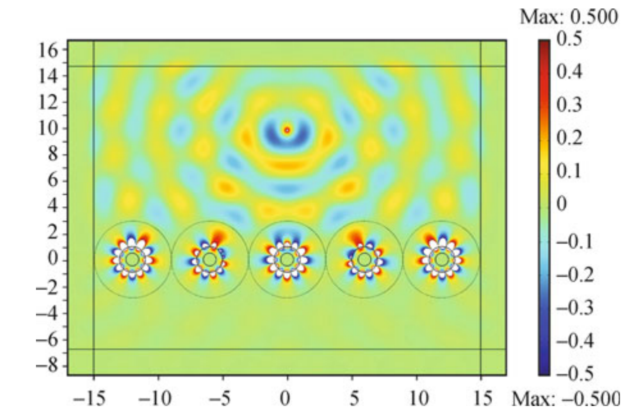

Fig. 5 The same as Fig. 4, but for an incident cylindrical wave with unit amplitude and frequency of 100 Hz, whose source is located at (0 m, 10 m).

4 Discussion and conclusions

Our proposed acoustic superscatterers make some applications possible, e. g., noise shielding and naval camouflage. A possible feature of superscatterer-based devices is the total scattering of incident acoustic waves while allowing the flow of air, fluids and/or particles. For instance, this feature can find its usage in the design of computers. In detail, cooling is an essential part of computers since the CPUs and graphic cards consume intensive power and dissipate more and more heat into the surrounding air. Currently a typical computer has a grid-like opening at the frontside and rearside of the chassis to form an air-flow passage. One of the negative effects of such a design is the leakage of noises produced by fans. If one coats the frame of the grid-like opening with a layer of acoustic metamaterials appropriately, to form superscatterers with equivalent scattering cross sections closely adjacent to each other, the noise would have no chance to escape from the chassis, while the air flow (or cooling) remains. Figure 4 shows a model demonstration for such a function in the presence of an incident acoustic plane wave with unit amplitude and frequency of 100 Hz. In this figure, a line of five cylindrical acoustic superscatteres are placed to shield the acoustic wave. The material parameters of the shells are determined according to Eqs. (5)–(8). As a result, the total reflection of the incident acoustic wave comes to appear, thus realizing noise shielding. Similar behavior appears for an incident cylindrical acoustic wave, as shown in Fig. 5. Another case of noise shielding arising from such acoustic superscatterers can be imagined for freeways, whose underlying mechanism keeps the same as shown by Figs. 4 and 5. The low-frequency noise produced by vehicles poses great danger to the health of residents living beside the freeways. If the lampstandards are surrounded with such a layer of acoustic metamaterials appropriately, noises would be kept inside the side of freeways.

As to naval camouflage, our proposal may be as follows, in view of the fact that both ultrasound spectroscopies and sonars depend on the scattering of acoustic waves at interfaces between different media. To confuse/mislead the enemy, one might coat a buoy with specific acoustic metamaterials, so that its scattering cross section is similar to that of a genuine submarine.

In fact, much more application examples can be proposed on the same footing as mentioned above. Nevertheless, we have to mention that our simulations reported in this work have been performed for one single frequency only. To achieve real applications, further study must be done, based on the fact that noises always contain a continuous spectrum of acoustic frequencies. On the other hand, the extension of this work to the case of thermal waves is also possible because of the recent achievement of thermal cloaks designed through the coordinate transformation method [30].

In summary, inspired by the pioneering work on electromagnetic superscatterers by Ma and his coworkers [11, 12, 14], we have convincingly revealed a path to enlarge the acoustic scattering cross section of embedded objects coated with acoustic metamaterials, which causes the coated object to behave as a scatterer bigger than its physical size. A model circular cylindrical superscatterer has been theoretically designed with accuracy. And its enhanced scattering properties have been Proved with full wave simulations based on the finite element method. It has been further adopted to realize a total scattering of acoustic waves while allowing the flow of air, fluids and/or particles, if any. This work presents a promising way to achieve various applications like noise shielding and naval camouflage.

Acknowledgements We thank Professor S. A. Cummer for his helpful advice, and are indebted to Ms. Z. W. Chang and Ms. Y. F. Pan for their assistance in plotting the figures. We also acknowledge the financial support from the National Natural Science Foundation of China (Grant Nos. 10874025 and 11075035) and the National Key Basic Research Special Fund of China (Grant No. 2011CB922004).

References

1. U. Leonhardt, Science, 2006, 312(5781): 1777
2. J. B. Pendry, D. Schurig, and D. R. Smith, Science, 2006, 312(5781): 1780
3. D. Schurig, J. J. Mock, B. J. Justice, S. A. Cummer, J. B. Pendry, A. F. Starr, and D. R. Smith, Science, 2006, 314(5801): 977
4. W. Cai, U. K. Chettiar, A. V. Kildishev, and V. M. Shalaev, Nat. Photonics, 2007, 1(4): 224
5. X. F. Xu, Y. J. Feng, L. Zhao, T. Jiang, C. H. Lu, and Z. Z. Xu, J. Phys D, 2008, 41: 215504
6. Y. Luo, J. J. Zhang, H. S. Chen, and B. I. Wu, J. Phys. D, 2008, 41: 235101
7. W. X. Jiang, T. J. Cui, G. X. Yu, X. Q. Lin, Q. Cheng, and J. Y. Chin, J. Phys. D, 2008, 41: 085504
8. Q. Wu, K. Zhang, F. Y. Meng, and L. W. Li, J. Phys. D, 2009, 42: 035408
9. D. Bao, E. Kallos, W. X. Tang, C. Argyropoulos, Y. Hao, and T. J. Cui, Front. Phys. China, 2009, 5(3): 319
10. Y. Lai, J. Ng, H. Y. Chen, Z. Q. Zhang, and C. T. Chan, Front. Phys. China, 2010, 5(3): 308
11. T. Yang, H. Chen, X. Luo, and H. Ma, Opt. Express, 2008, 16(22): 18545
12. X. Luo, T. Yang, Y. Gu, and H. Ma, arXiv:0809.1823v1, 2008
13. http://www.nature.com/news/2008/080919/full/news. 2008. 1113.html
14. H. Chen, X. Zhang, X. Luo, H. Ma, and C. T. Chan, New J. Phys., 2008, 10(11): 113016
15. Z. Liu, X. Zhang, Y. Mao, Y. Y. Zhu, Z. Yang, C. T. Chan, and P. Sheng, Science, 2000, 289(5485): 1734
16. J. Mei, Z. Liu, W. Wen, and P. Sheng, Phys. Rev. B, 2007, 76(13): 134205
17. Z. Liu, C. T. Chan, and P. Sheng, Phys. Rev. B, 2005, 71(1): 014103
18. K. M. Ho, C. K. Cheng, Z. Yang, X. X. Zhang, and P. Sheng, Appl. Phys. Lett., 2003, 83(26): 5566
19. Z. Liu, C. T. Chan, P. Sheng, A. Goertzen, and J. Page, Phys. Rev. B, 2000, 62(4): 2446
20. J. Mei, Z. Liu, W. Wen, and P. Sheng, Phys. Rev. Lett., 2006, 96(2): 024301
21. Z. Yang, J. Mei, M. Yang, N. H. Chan, and P. Sheng, Phys. Rev. Lett., 2008, 101(20): 204301
22. H. Chen and C. T. Chan, Appl. Phys. Lett., 2007, 91(18): 183518
23. S. A. Cummer and D. Schurig, New J. Phys., 2007, 9(3): 45
24. N. Fang, D. Xi, J. Xu, M. Ambati, W. Srituravanich, C. Sun, and X. Zhang, Nat. Mater., 2006, 5(6): 452
25. S. H. Lee, C. M. Park, Y. M. Seo, Z. G. Wang, and C. K. Kim, J. Phys.: Condens. Matter, 2009, 21(17): 175704
26. B. Liu and J. P. Huang, Commun. Theor. Phys., 2010, 53: 560
27. Q. Su, B. Liu, and J. P. Huang, Front. Phys., 2011, 6(1): 65
28. J. Li and C. T. Chan, Phys. Rev. E, 2004, 70(5 Pt 2): 055602
29. D. Schurig, J. B. Pendry, and D. R. Smith, Opt. Express, 2006, 14(21): 9794
30. C. Z. Fan, Y. Gao, and J. P. Huang, Appl. Phys. Lett., 2008, 92(25): 251907